

convergence of the SCF procedure was also observed in this study at allenic geometries (e.g., 82 iterations at point 2 of Table I using a carbene-like initial guess for the wave function). The SCF results for linear geometries corresponding to points 2, 3, 4, 5, and 7 of Table I were examined further by requiring stricter convergence (difference of the square of the coefficients less than 1×10^{-8}) and by using three initial guess vectors (a carbene-like vector from point 3, a nitrene-like vector from point 3, and diagonalization of the one-electron Hamiltonian) for each point. The choice of orbitals with which to perform the CI was also examined by means of iterative natural orbital CI calculations on these points. All single and double valence excitations were allowed as described above as CI14.

For points 2, 4, 5, and 7 only one SCF energy (see Table I) was obtained with the various initial guesses at the MO. As noted, the convergence at point 2 was remarkably slow. For point 3, two distinct SCF solutions were obtained. The lower SCF energy ($-130.578\ 374$) was calculated using either the diagonalized one-electron Hamiltonian or the nitrene vector initial guesses. When a carbene initial guess was employed an SCF energy of $-130.576\ 445$ was obtained for what is almost certainly a fully converged iterative process (difference square coefficients 0.79×10^{-8}). A consideration of the highest two occupied MOs of the two SCF wave functions indicates that the final result for this allenic geometry retains the character of the initial guess. Thus the higher energy SCF wave function is of carbene and the lower energy result of nitrene character.

The INO-CI energy results are given in Table VII. For points 4, 5, and 7, the first iteration of the NO procedure yielded the lowest energy indicating that the SCF-MO provide a suitable set of correlating orbitals. However, for points 2 and 3, which most resemble allenic structures, several cycles of the INO procedure lead to lower energies. For point 3, the higher carbene SCF solution more rapidly reaches a minimum energy than does the lower SCF energy nitrene solution.

Thus, the electronic structure of HCCN is somewhat bizarre in the region of linear allenic geometries. This observation notwithstanding, it seems clear that at the level of theory reported here, no combination of alternate SCF solutions with natural orbital iterations leads to an energy lower than that of

the conventional bent cyanocarbene. Therefore, it may be concluded that, although correlation effects significantly *flatten* the predicted Hartree-Fock potential energy surface, the qualitative SCF geometrical prediction of a bent cyanocarbene structure for HCCN remains valid.

Acknowledgments. M.E.Z. wishes to thank Morgan Conrad for many helpful discussions concerning quantum chemistry and computational methods. The collaboration leading to this paper was made possible through a sabbatical grant to M.E.Z. from Wichita State University. This work was supported by the National Science Foundation (Grant CHE-762261).

References and Notes

- (1) (a) Wichita State University; (b) University of California.
- (2) (a) A. Dendramis, J. F. Harrison, and G. E. Leroi, *Per. Bunsenges. Phys. Chem.*, **82**, 7 (1978); (b) J. F. Harrison, A. Dendramis, and G. E. Leroi, *J. Am. Chem. Soc.*, **100**, 4352 (1978).
- (3) R. A. Bernheim, R. J. Kempf, P. W. Humer, and P. S. Skell, *J. Chem. Phys.*, **41**, 1156 (1964); R. A. Bernheim, R. J. Kempf, J. V. Gramas, and P. S. Skell, *ibid.*, **43**, 196 (1965); R. A. Bernheim, R. J. Kempf, and E. F. Reichenbecher, *J. Magn. Reson.*, **3**, 5 (1970).
- (4) E. Wasserman, W. A. Yager, and V. J. Kuck, *Chem. Phys. Lett.*, **7**, 409 (1970).
- (5) A. Dendramis and G. E. Leroi, *J. Chem. Phys.*, **66**, 4334 (1977).
- (6) R. Hoffmann, G. D. Zeiss, and G. V. Van Dine, *J. Am. Chem. Soc.*, **90**, 1485 (1968).
- (7) C. W. Bauschlicher, H. F. Schaefer, and P. S. Bagus, *J. Am. Chem. Soc.*, **99**, 7106 (1977).
- (8) N. C. Baird and K. F. Taylor, *J. Am. Chem. Soc.*, **100**, 1333 (1978).
- (9) R. R. Lucchese and H. F. Schaefer, *J. Am. Chem. Soc.*, **99**, 13 (1977).
- (10) (a) S. Huzinaga, *J. Chem. Phys.*, **42**, 1293 (1965); (b) T. H. Dunning, *ibid.*, **53**, 2823 (1970); (c) T. H. Dunning and P. J. Hay in "Modern Theoretical Chemistry", Vol. 3, H. F. Schaefer, Ed., Plenum Press, New York, 1977.
- (11) P. K. Pearson, R. R. Lucchese, W. H. Miller, and H. F. Schaefer in "Mini-computers and Large Scale Computations", ACS Symposium Series No. 57, American Chemical Society, Washington, D.C., 1977; H. F. Schaefer and W. H. Miller, *Comput. Chem.*, **1**, 85 (1977).
- (12) D. B. Neumann, H. Basch, R. L. Kornegay, L. C. Snyder, J. W. Moskowitz, C. Hornback, and S. P. Liebmann, "POLYATOM 2", Program No. 199, Quantum Chemistry Program Exchange, Indiana University, Bloomington, Ind., 1972.
- (13) F. W. Bobrowicz and W. A. Goddard in ref 10c.
- (14) R. R. Lucchese and H. F. Schaefer, *J. Chem. Phys.*, **68**, 769 (1978); R. R. Lucchese, B. R. Brooks, J. H. Meadows, W. C. Swope, and H. F. Schaefer, *J. Comput. Phys.*, **26**, 243 (1978).
- (15) M. E. Zandler, *Chem. Phys. Lett.*, to be submitted.
- (16) Program SPLSQUAD was developed and implemented in BASIC on the COMMODORE PET. Cassette copies of this program are available from M.E.Z. for a nominal fee.
- (17) We thank Mr. D. Reuter for performing the normal coordinate analysis.

Determination and Analysis of the Formic Acid Conformational Hypersurface

Michael R. Peterson and Imre G. Csizmadia*

Contribution from the Department of Chemistry, University of Toronto, Toronto, Ontario, Canada M5S 1A1. Received May 8, 1978

Abstract: An analytical conformational hypersurface was fitted to a total of 64 ab initio SCF energy points for formic acid. The geometries of the syn and anti minima, and the OH rotation and C-O-H in-plane inversion saddle points, were determined from the hypersurface. The syn and anti structures, as well as the saddle point for tautomerization (H transfer), were also found directly by complete geometry optimization.

A topic of considerable interest is the interdependence of isomerization or tautomerization and conformational change. Although it is traditional to discuss these processes as independent phenomena, in effect they represent different cross sections of the same energy hypersurface. Perhaps the justifi-

cation for the separation of these processes lies in the difference in barrier heights, but sometimes certain conformational transition states may also have relatively high energies. This situation occurs for methanol, for which the barrier to OH rotation has been calculated¹ to be 1.44 kcal/mol, while the

Table I. Syn–Anti Energy Difference and Barrier to OH Rotation for Formic Acid

ΔE , kcal/mol ^a	ΔE_1 , kcal/mol ^b	ref
	Experimental	
2.0	17	10
	10.9 (98°)	11
	13.4	12
>4		13
	Theoretical	
8.1		14
9.46	14.20	15
8.1	13.0	16
6.3	12.2 (97°)	17
4.8	12.34	18

^a Syn–anti energy difference. ^b Energy difference between TS₁ and S (barrier height for rotation). The torsional angle τ of TS₁ is indicated in parentheses, if not assumed to be 90°.

barrier to in-plane inversion at oxygen was 32.5 kcal/mol. The inversion barrier for water was computed¹ to be 31.1 kcal/mol.

A molecule that possesses rotational, in-plane inversion and tautomerization barriers is formic acid, as illustrated by Scheme I.

Table I collects previous experimental and theoretical data for the syn–anti energy difference (ΔE) and the barrier (ΔE_1) to OH rotation (path 1, through TS₁). The barrier to in-plane inversion (ΔE_2) may be estimated from water and methanol¹ to be 30–35 kcal/mol, while TS₃ has been calculated² to lie 74.2 kcal/mol above the syn (S) conformation. This situation is illustrated in Figure 1, using the notation of Scheme I.

The geometrical parameters used to define the hypersurface are the O–H bond length (r), the C–O–H angle (α), and the O=C–O–H torsional angle (τ), and all the critical points from Scheme I lie on this hypersurface.

The portion of the hypersurface involved in paths 1 and 2 can readily be described in terms of r , α , and τ , but a transformation of the hypersurface coordinates suitable for path 3, including the C_{2v} symmetry of TS₃, has not yet been found. Here, then, we report a mathematical fit of the conformational portion of the formic acid hypersurface, and the determination of the geometries of TS₁ and TS₂, which cannot be obtained by direct energy optimization.

Method

The structures of syn, anti, and linear (which should approximate TS₂) formic acid were determined by minimal basis set *ab initio* calculations,³ with complete geometry optimization. Sixty-one more points were generated by varying the O–H bond length (r) between 0.91 and 1.10 Å, the C–O–H bond angle (α) between 90 and 210°, and the O=C–O–H torsional angle (τ) from 0 to 180° to systematically cover the entire hypersurface coordinate space. For each of these latter 61 points, the C=O and C–O bond lengths and the O=C–O angle were optimized. The C–H bond length and O=C–H angle were fixed at 1.106 Å and 124°, respectively, based on the results of the complete geometry optimizations. Also, to maintain planarity at the carbon atom, the O–C–H angle was decreased by 1° for every 1° increase in the O=C–O angle during the optimization.

An analytical equation of the form

$$E = E(r, \alpha, \tau) = \sum_i C_i f_i(r) g_i(\alpha) h_i(\tau) \quad (1)$$

where each term is a product of three functions, one for each of the coordinates r , α , and τ , was fitted to the 64 points by a least-squares stepwise regression technique.⁴ Polynomials in

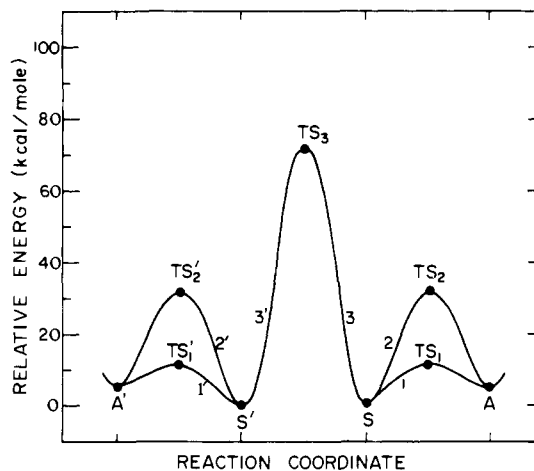
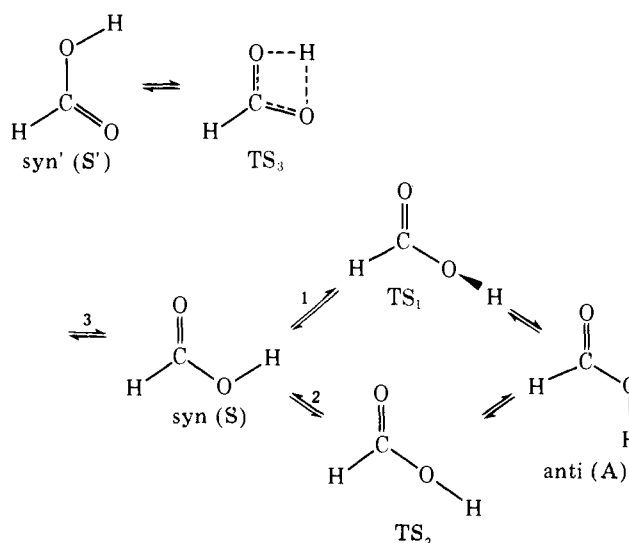


Figure 1. Projected energy profile for the total conformational (processes $S = A$, $S' = A'$) and tautomerization (process $S = S'$) hypersurface of formic acid. The structures and pathways are labeled as in Scheme I.

Scheme I. Critical Points of the Formic Acid Hypersurface



$(r - 0.99)^n$ were used for f_i , and truncated Fourier series for g_i and h_i .

Results and Discussion

The optimized geometries of the syn, anti, and linear structures are given in Table II. As expected, the HC(=O)O moiety was planar for all three conformers. The syn geometry agrees fairly well with the experimental gas-phase structures listed in Table III, except that the C–O bond is somewhat longer than the more recent microwave results. Our optimum geometry is very close to that obtained by Del Bene et al.,⁵ the first QM entry in Table III, using the same basis set.

The calculated syn–anti energy difference (ΔE) was 4.5 kcal/mol, comparable to the experimental values of Table I, and smaller than the previous *ab initio* results. The barrier heights for rotation of the hydroxyl group and inversion at oxygen (through a linear C–O–H bond) can only be estimated, as these critical points⁷ cannot be determined by minimization of the energy. To locate these transition states, an analytical hypersurface fitted to the points was searched for its critical points.

The terms and linear coefficients of eq 1 are detailed in Table IV. The average error of the fit was 0.014 kcal/mol (the root mean square error was 0.020 kcal/mol), and the largest

Table II. Optimized Geometries of Formic Acid Conformers (Bond Lengths in Ångstroms, Angles in Degrees)

conformer	C=O	C-O	C-H	O-C-O	O=C-H	O-C-H	O-H	C-O-H	E, hartrees
syn ^a	1.214	1.378	1.102	124.2	125.5	110.3	0.991	105.4	-186.217 80
anti ^b	1.211	1.382	1.108	121.4	123.4	115.2	0.988	106.4	-186.210 70
linear	1.215	1.316	1.109	123.7	124.3	112.0	0.952	180.0 ^c	-186.131 99

^a The O=C-O-H torsional angle was fixed at 0°. ^b The O=C-O-H torsional angle was fixed at 180°. ^c The C-O-H angle was fixed at 180°.

Table III. Experimental Gas-Phase and Theoretical Structures of Syn Formic Acid

method ^a	C=O ^b	C-O ^b	C-H ^b	O-C-O ^c	O=C-H ^c	O-C-H ^c	O-H ^b	C-O-H ^c	ref
ED	1.24	1.42		117.					19
ED	1.213	1.368		123.5					20
IR	1.225	1.41		125.	122.	113.		107.	21
ED	1.23	1.36		122.4			0.97		22
MW	1.22	1.34	1.09	124.8	121.7	113.5	0.97	105.5	23
MW	1.245	1.312	1.085	124.3			0.95	107.8	10
MW	1.202	1.343	1.097	124.9	124.1	111.0	0.972	106.3	24
MW	1.237	1.312	1.092	125.0	121.0	114.0	0.961	107.8	25
ED	1.217	.361	1.106	123.4	127.5	109.1	0.984	107.3	26
MW	1.228	1.317	1.097	125.0	124.6	110.4	0.974	106.8	27
QM	1.214	1.386	1.104	123.7	125.9	110.4	0.991	104.8	5
QM	1.215	1.332	1.085				0.97	114.	6

^a Experimental methods used were electron diffraction (ED), infrared spectroscopy (IR), and microwave spectroscopy (MW). QM refers to ab initio quantum chemical structure prediction. ^b Measured in Ångstroms. ^c Measured in degrees.

Table IV. Formic Acid Analytic Hypersurface Equation^a

term	$f_i(r)$	$h_i(\tau)^b$	C_i^c	std error ^d
1	1	1	142.352	1.359
2	$r - 0.99$	1	75.112	1.081
3	$(r - 0.99)^2$	1	730.793	4.890
4	$(r - 0.99)^3$	1	480.235	93.560
5	1	$(\sin \alpha)^2$	-130.079	1.357
6	$r - 0.99$	$(\sin \alpha)^2$	-88.570	1.223
7	1	$(\sin 2\alpha)^2$	-5.675	0.158
8	$r - 0.99$	$(\sin 2\alpha)^2$	-17.872	1.105
9	$(r - 0.99)^3$	$(\sin 2\alpha)^2$	-587.811	132.736
10	1	$\cos \alpha$	77.940	1.049
11	$(r - 0.99)^3$	$\cos \alpha$	1349.907	164.122
12	1	$\cos 3\alpha$	9.310	0.304
13	$r - 0.99$	$\cos 3\alpha$	13.218	0.607
14	1	$\sin \alpha$	-3.360	0.099
15	$r - 0.99$	$\sin \alpha$	-0.984	0.265
16	$(r - 0.99)^3$	$\sin \alpha$	-864.179	79.527
17	1	$\sin 2\alpha$	-1.680	0.129
18	1	$\sin 3\alpha$	-1.320	0.093
19	1	$\sin 4\alpha$	-0.175	0.038
20	$r - 0.99$	$\sin 4\alpha$	1.280	0.206
21	1	$\sin 2\alpha$	6.101	0.215
22	1	$\sin 3\alpha$	6.962	0.251
23	1	$\sin 4\alpha$	1.937	0.076
24	1	$(\sin \alpha)^2$	3.826	0.254
25	$r - 0.99$	$(\sin \alpha)^2$	3.058	0.166
26	1	$(\sin 2\alpha)^2$	-3.846	0.088
27	$(r - 0.99)$	$(\sin 2\alpha)^2$	-3.260	0.201
28	$(r - 0.99)^3$	$\sin 3\alpha$	455.938	23.738
29	1	$\sin 4\alpha$	0.051	0.010
30	1	$(\sin \alpha)^2$	-0.712	0.015
31	1	$(\sin 2\alpha)^2$	0.238	0.009
32	1	$(\sin \alpha)^2$	-0.082	0.008
33	1	$(\sin 2\alpha)^2$	0.071	0.014
34	$(r - 0.99)^2$	$(\sin 2\alpha)^2$	-20.904	7.631

^a Each term in the equation is a product of three functions $f_i(r)$, $g_i(\alpha)h_i(\tau)$, one for each coordinate. ^b Note that only $\cos n\tau$ was used owing to the rotational symmetry about $\tau = 0^\circ$. ^c These coefficients calculate $E(r, \alpha, \tau)$ in kcal/mol relative to the energy of the optimized syn conformer. ^d Standard error of the coefficient.

Table V. Coordinates and Energies (kcal/mol) of the Critical Points of the Formic Acid Hypersurface

conformer	$r, \text{Å}$	α, deg	τ, deg	$\Delta E(\text{fitted})^a$	$\Delta E(\text{ab initio})^b$
syn (S)	0.990	104.7	0.0	0.00	0.00 ^c
anti (A)	0.990	105.7	180.0	4.36	4.46 ^c
TS ₁	0.993	104.8	89.7	9.55	9.61 ^d
TS ₂	0.950	180.8	0.0	53.82	53.85 ^e

^a Measured relative to the energy of the syn conformer from eq 1. ^b Measured relative to the energy of the optimized syn conformer from Table II. ^c At the geometry from Table II. ^d For the point $(r, \alpha, \tau) = (0.990, 105.0^\circ, 90.0^\circ)$. ^e At the linear geometry from Table II.

deviation was 0.06 kcal/mol. Thus the hypersurface equation should accurately follow the true ab initio hypersurface, which was confirmed by examining plots of various cross sections of the fitted hypersurface. All terms are significant (i.e., different from zero) at the 1% confidence level.

Two notes should be made concerning the form of the equation: for a linear C-O-H angle ($\alpha = 180^\circ$), there is a line of degeneracy (constant energy) in the τ subspace, which is incorporated into the equation. Terms 1-13 have no τ dependence for all values of α , and terms 14-34 are identically zero when α is 180° . Also, since $(r - 0.99)$ is in the range 0.0-0.1, terms with $(r - 0.99)^2$ and $(r - 0.99)^3$ for $f_i(r)$ are effectively multiplied by factors of the order 0.005 and 0.0005, respectively, accounting for the large coefficients for those terms.

The minima of the analytic equation were found directly using a variable metric optimization technique.⁸ The saddle points were determined by minimizing⁸ the squared gradient length⁹ Sg:

$$Sg = \left(\frac{\partial E}{\partial r}\right)^2 + \left(\frac{\partial E}{\partial \alpha}\right)^2 + \left(\frac{\partial E}{\partial \tau}\right)^2 \quad (2)$$

which is zero at a critical point. The order of the critical point was then determined from the number of negative eigenvalues of the Hessian matrix H which has elements

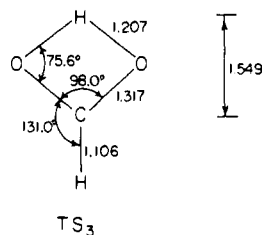


Figure 2. Optimized geometry of the saddle point for tautomerization (TS_3). The symmetry was constrained to be C_{2v} . All interatomic distances are measured in ångströms.

$$H_{ij} = \frac{\partial^2 E}{\partial q_i \partial q_j} \quad (3)$$

where the q 's each refer to one of r , α , or τ . Minima are zero-order critical points; saddle and supersaddle points have orders 1 and 2, respectively.

Table V contains the coordinates and relative energies of the critical points of the analytic hypersurface. The hydroxyl rotation saddle point (TS_1) occurs very near $\tau = 90^\circ$ (perpendicular), and as r and α vary only slightly between the syn and anti minima, path 1 corresponds to essentially rigid rotation. The linear structure (TS_2) is actually a supersaddle point (order 2) and is predicted to lie quite close to the optimized linear geometry. The geometries and relative energies determined from the analytic equation compare favorably with those obtained directly from ab initio calculation, as may be seen from Tables II and V.

The computed barrier to rotation (through TS_1) is a bit lower than the previous ab initio and experimental values, but the 54 kcal/mol barrier to in-plane inversion (through TS_2) is considerably higher than that of water or methanol (31–32.5 kcal/mol).¹

Although the entire tautomerization hypersurface was not determined, the geometry of TS_3 was optimized within the C_{2v} symmetry, and is shown in Figure 2. Thus the barrier to tautomerization is 59 kcal/mol, considerably lower than the 74 kcal/mol computed previously² using the same basis set. Figure 3 collects all the calculated results, and is comparable with Figure 1, the estimated results.

The values of ΔE and ΔE_1 are likely reliable to within a few kilocalories per mole, as suggested by the experimental results. However, ΔE_2 and ΔE_3 (through TS_2 and TS_3) may contain errors of 5–10 kcal/mol as the minimal basis set may not have sufficient flexibility to describe these nonequilibrium geometries. Despite these systematic errors, more figures are included in Table V so the small differences between the analytic equation and direct determination approaches are visible.

In conclusion it perhaps should be emphasized that the conventionally accepted notion that barriers along reactive coordinates of a hypersurface are always considerably higher than barriers along conformational coordinates of the same hypersurface (cf. Figure 3) need not necessarily be always true. The present results (tautomerizational barrier 59 kcal/mol, in-plane inversion 54 kcal/mol) with a difference of 5 kcal/mol in barrier heights would tend to support this conclusion.

Acknowledgments. We are indebted to the National Research Council of Canada for continuous financial support. One of us (M.R.P.) would like to thank the National Research

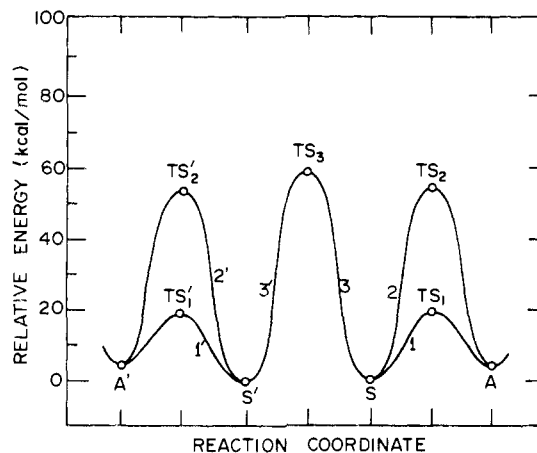


Figure 3. Computed energy profile for the total conformational and tautomerization hypersurface, using the notation of Scheme I.

Council of Canada for the award of a Postgraduate Scholarship.

References and Notes

- (1) L. M. Tel, S. Wolfe, and I. G. Csizmadia, *J. Chem. Phys.*, **59**, 4047 (1973).
- (2) J. Koller, D. Hadzi, and A. Azman, *J. Mol. Struct.*, **17**, 157 (1973).
- (3) All calculations were performed with the GAUSSIAN 70 program system: W. J. Hehre, W. A. Lathan, R. Ditchfield, M. D. Newton, and J. A. Pople, Program 236, Quantum Chemistry Program Exchange Catalog, Vol. 10, Department of Chemistry, Indiana University, Bloomington, Ind., 1974. The STO-3G basis set used is described in W. J. Hehre, R. F. Stewart, and J. A. Pople, *J. Chem. Phys.*, **51**, 2657 (1969).
- (4) Statistical Analysis System (SAS 76): A. J. Barr, J. H. Goodnight, J. P. Sall, and J. T. Helwig, SAS Institute Inc., P.O. Box 10066, Raleigh, N.C. 27605.
- (5) J. E. Del Bene, G. T. Worth, F. T. Marchese, and M. E. Conrad, *Theor. Chim. Acta*, **36**, 195 (1975).
- (6) P. Bosì, G. Zerbi, and E. Clementi, *J. Chem. Phys.*, **66**, 3376 (1977).
- (7) A critical point is one where the gradient of the energy with respect to every coordinate q_i (Cartesian or internal) is zero:

$$\frac{\partial E}{\partial q_i} = 0$$
- (8) W. C. Davidson, "Variable Metric Method for Minimization", AEC Research and Development Report ANL-5990 (revised), 1959. We thank P. G. Mezey for the use of his computer program implementing the method.
- (9) J. W. McIver, Jr., and A. Kormornicki, *J. Am. Chem. Soc.*, **94**, 2625 (1972).
- (10) R. G. Lerner, B. P. Dailey, and J. P. Friend, *J. Chem. Phys.*, **26**, 680 (1957).
- (11) T. Miyazawa and K. S. Pitzer, *J. Chem. Phys.*, **30**, 1076 (1959).
- (12) D. L. Bernitt, K. O. Hartman, and I. C. Hisatsune, *J. Chem. Phys.*, **42**, 3553 (1965).
- (13) D. R. Lide, Jr., *Trans. Am. Crystallogr. Assoc.*, **2**, 106 (1966).
- (14) P. Ros, *J. Chem. Phys.*, **49**, 4902 (1968).
- (15) A. C. Hopkinson, K. Yates, and I. G. Csizmadia, *J. Chem. Phys.*, **52**, 1784 (1970).
- (16) M. E. Schwartz, E. F. Hayes, and S. Rothenberg, *J. Chem. Phys.*, **52**, 2011 (1970).
- (17) L. Radom, W. A. Lathan, W. J. Hehre, and J. A. Pople, *Aust. J. Chem.*, **25**, 1601 (1972).
- (18) M. Perricaudet and A. Pullman, *Int. J. Pept. Protein Res.*, **5**, 99 (1973).
- (19) J. Karle and L. O. Brockway, *J. Am. Chem. Soc.*, **66**, 574 (1944).
- (20) V. Schomaker and J. M. O'Gorman, *J. Am. Chem. Soc.*, **69**, 2638 (1947).
- (21) V. Z. Williams, *J. Chem. Phys.*, **15**, 232 (1947).
- (22) I. L. Karle and J. Karle, *J. Chem. Phys.*, **22**, 43 (1954).
- (23) R. Trambarulo and P. M. Moser, *J. Chem. Phys.*, **22**, 1622 (1954).
- (24) G. H. Kwei and R. F. Curl, Jr., *J. Chem. Phys.*, **32**, 1592 (1960).
- (25) A. M. Mirri, *Nuovo Cimento*, **18**, 849 (1960).
- (26) A. Almennigen, O. Bastiansen, and T. Motzfeldt, *Acta Chem. Scand.*, **23**, 2848 (1969).
- (27) J. Bellet, A. Deldalle, C. Samson, G. Steenbeckelers, and R. Wertheimer, *J. Mol. Struct.*, **9**, 65 (1971).